ISSN 2522-9400 **European Modern Studies Journal** *Vol 9 No 1*
available at www.journal-ems.com
DOI: 10.59573/emsj.9(1).2025.6

Numerical Solution of the System of Non-Linear Differential Equations of the Three-Body Problem in a Special Case

Azem Hysa[1]*, M.S. Priyadarshini[2], Mohamed Metwally Mahmoud[3]
[1]Department of Applied and Natural Sciences, "Aleksander Moisiu" University, Neighborhood 1, Currilave Street, Durres, 2001, Albania
[2]Department of Electrical and Electronics Engineering, K.S.R.M College of Engineering (Autonomous), Kadapa 516005, India
[3]Electrical Engineering Department, Faculty of Energy Engineering, Aswan University, Aswan 81528, Egypt

Abstract. The aim of this study is to numerically integrate the system of non-linear differential equations of the three-body problem in a special case. The objective of the present study is to find a lunar trajectory, a manifold and to construct the Poincaré section and reconstruction of the phase space in $\mathbb{R}^2$ for the Earth-Moon system. Then applying this model to exoplanetary systems, we find different types of orbits for a test astrophysical object in a binary star system.

In this paper, we will first present a review of the three-body problem in the context of both historical and modern developments. To achieve the objectives of this study, we have performed a large number of numerical tests in MATLAB® 2024 b software by numerical integration of the nonlinear system equations of motions given by Newton's and Hamilton's methods. From these numerical tests, we have obtained some interesting results inside solar system and an exoplanetary system. All the results of this study are original and were calculated in the software MATLAB® 2024 b. This software is very powerful in graphics.

Keywords: Poincaré section, lunar trajectory, phase space, three-body problem, exoplanetary system

1. Introduction

The observation of the sky and theoretical studies related to the movement of celestial bodies have been done for a long time and the sciences such as Celestial Mechanics and Astronomy was created a long time ago. Several of the most important names in history are related to this field, like Ptolomeus, Nicolaus Copernicus, Galileo Galilei, Johannes Kepler, Isaac Newton, Euler, Lagrange, Albert Einstein and others, who helped to find the physical laws that govern those motions (Bertachini et al., 2013). The combination of theory and practical observations created new sciences such as Astrodynamics, Astrophysics, etc. This combination, also showed the existence of planetary systems around other stars, the so called "exoplanets." Soon "exomoons" around those "exoplanets" will be found (Bertachini et al., 2013).

The case of two gravitationally interacting celestial bodies can be fully solved, and was solved by Newton (1687) earlier on in the 17th century (Newton, 1687). How are the orbits of three-point masses that are attracted to each other by Newton's Laws of Motion and Newton's Law of Universal Gravitation? This is the so-called "general three-body problem". This problem can be traced back to Newton in 1687, but quite a few families of periodic orbits were found 300 years thereafter (Liao et al., 2022). The classical three-body problem is formulated in an attempt to understand the effect of the Sun on the Moon's Keplerian orbit around the

* Corresponding Author

Earth. It has attracted the attention of some of the best physicists and mathematicians and led to the discovery of 'chaos' (Krishnaswami & Senapat, 2019).

The dynamic of this problem is non-linear, very complex, and it becomes extremely difficult to find periodic orbits but scientists have found methods to study this system. In the 300 years since this problem was first recognized, just three families of solutions have been found. Euler reported one in 1740, Lagrange in 1772, and More in 1993 (this was later confirmed in 2000 by Chenciner and Montgomery, 2000). Why is so difficult to find periodic orbits of three-body systems? The mysterious reasons were revealed by Poincaré (Poincaré 1890), who proved that, unlike the two-body problem that is integrable and thus its solutions are completely understood, the three-body problem is not integrable, and the trajectories of three-body systems are generally rather sensitive to initial conditions. These trajectories are chaotic, i.e. non-periodic, as discovered by Poincaré in 1890 and confirmed again by Lorenz in 1963 and Stone & Leigh in 2019.

At the time Poincaré lived, the computer had not yet been discovered. The discovery of the computer and the development of numerical methods brought new innovations in the study of analytically unsolvable problems, such as the problem of many bodies. In 2015, Hudomal discovered 14 new families of periodic solutions (Hudomal, 2015). It is a feat in Mathematical Physics, and it could conceivably help astrophysicists understand new planetary systems. The new solutions were discovered when researchers at Shanghai Jiaotong University China tested 16 million different trajectories using a supercomputer. In 2017, Xiaoming, Yipeng, and Shijun presented 1349 families of Newtonian periodic planar three-body orbits with unequal mass and zero angular momentum and the initial conditions in this case of isosceles collinear configurations. Among these 1223 families are entirely new (Xiaoming, Yipeng, & Shijun, 2017). All the new orbits found are periodic. In 2023, Hristov et al. (2023) discovered 12409 solutions.

In the digital age, the behavior of non-integrable systems is usually and primarily studied with restricted models or coupled with the help of numerical integrators. Over time, these numerical integrators progressed, and the numerical challenge led to the introduction of many new techniques (Szücs, 2023). The question is, which numerical algorithm to choose for the correct research (Szücs, 2023)? In the paper with topic: Overview–regularization and numerical methods in Celestial Mechanics and Dynamical Astronomy (Szücs, 2023) are presented some analytical and numerical methods with highly accurate computations, such as regularization methods and symplectic integrators, which can be useful in obtaining the corresponding more accurate results.

Some, important mathematical aspects for new Regularization of the Restricted Three-Body Problem (RTBP) and Regularization of the Circular Restricted Three-Body Problem (CRTBP) using "similar" coordinate systems have been presented by authors Roman, Szücs, 2011, 2012. Also, in 2014, Roman, and Szücs, presented a family of zero-velocity curves in the restricted three-body problem. Regularized equations of motion can improve numerical integration for the propagation of orbits, and i.e. simplify the treatment of mission design problems.

In this study we present the motion of a test astrophysical body within same exoplanetary systems.

We focus on the Circular Restricted Three-Body Problem (CRTBP), which can be applied to the Earth-Moon system with a spacecraft, the Sun-Earth-moon system, the Sun-Jupiter system with an asteroid etc. In the exoplanetary system this problem can be applied to a single star with giant and terrestrial exoplanet, a single star with a giant exoplanet and exomoon and also in binary stellar systems with a giant or terrestrial exoplanet or a test exomoon. One of the most extreme cases of the Circular Restricted Three-Body Problem involves the study of exoplanets orbiting either one or both components of a binary star system, in which the more massive and less massive stars are called the primary and secondary.

We will assume that the three bodies form an isolated system. This assumption is made so that there is no other external effect on the three-body system. Considering that the third body (an astrophysical object) is massless, then the problem in this case is said to be “Restricted” (Lizy-Destrez et al., 2019). Since the eccentricity of the planets around the sun is small, then we have the approximation that the two massive bodies in this problem move in circular orbits around the center of mass (Lei & Xu, 2013).

Some important results regarding the movement of a test particle under the action of the gravitational field of two massive bodies within our solar system and some exoplanetary systems have been presented in our previous work (Hysa, 2024; Hysa, Peqini, Hafizi, 2024).

2. Three Body Problem

We assume that we have N bodies with masses m_1, m_2,…, m_N, which interact through Newton’s law (Newton, 1687). Let $\mathbf{r}^{(i)} \in \mathbf{R}^3$, $i = 1,2,3, \ldots, N$, denote the position of the bodies in an inertial reference frame (Celleti, 2006). So, the equations of motion of the N-body problem can be written in the form (Newton, 1687, Celleti, 2006):

$$\ddot{\mathbf{r}}^{(i)} = -G \sum_{j=1, j \neq i}^{N} \frac{m_j\left(\mathbf{r}^{(i)} - \mathbf{r}^{(j)}\right)}{|\mathbf{r}^{(i)} - \mathbf{r}^{(j)}|^3} \tag{1}$$

For N=3, we have the general three-body problem (Celleti, 2006). The 18 phase space variables of the 3-body problem (components of $\mathbf{r}_1$, $\mathbf{r}_2$, $\mathbf{r}_3$, $\mathbf{p}_1$, $\mathbf{p}_2$, $\mathbf{p}_3$) satisfy 18 first order ordinary differential equations (ODEs) $\dot{\mathbf{r}}^{(i)} = \mathbf{p}^{(i)}$, $\dot{\mathbf{p}}^{(i)} = -\nabla_{\mathbf{r}^{(i)}} U$, where U-is the potential energy of the system. Lagrange’s reduction from 18 to 7 equations. Lagrange (1772) used the conservation laws to reduce these ODEs to a system of 7 first order ODEs (Govind and Himalaya, 2019). A special case is given by the Restricted Three-Body Problem (RTBP). Normalizing the gravitational constant G to 1. For N=3 and $m_3 = 0$ in Equation (1), we obtain this problem (Celleti, 2006).

For this problem, the equations of motion (1) have five special solutions that define the so-called Lagrange points (equilibrium points) (Szebehely, 1967). Lagrange points are points in a binary system on which the third body could reach equilibrium state. Three of them, L_1, L_2, and L_3 (collinear Lagrange points), are aligned with the primary and secondary masses, while the other two, L_4 and L_5 (triangular Lagrange points), form two equilateral triangles with the primary and secondary, respectively (Rebeca S. Ribeiro, de Melo, Prado, 2022).

The system of equations of motion (1) in the special case of the RTBP, admits a quantity that is conserved for any solution. This quantity is called the Jacobi constant or Jacobi integral and is given by:

$$C = 2\left[(x^2 + y^2) + \frac{1-\mu}{\sqrt{(x+\mu)^2 + y^2 + z^2}} + \frac{\mu}{\sqrt{(x+\mu-1)^2 + y^2 + z^2}} + \frac{1}{2}\mu(1-\mu)\right] - v^2, \tag{2}$$

where v – is the velocity of the test third body (Jacobi, 1836, Borcherds, 1996) and μ is a mass parameter of the system (Murray & Dermott, 1999). This quantity is very important because it plays the role of energy in this problem and is the only known conserved quantity for the CRTBP (Murray & Dermott, 1999). The equation (2) defines a set of surfaces for particular values of $C(x, y, z)$. These surfaces, known as *zero-velocity surfaces*, play an important role in placing bounds on the motion of the test third body (a test particle) (Lee, & Ahn, 2021, 2022, 2024).

This is the only known conserved quantity for the circular restricted three-body problem. This integral is used to derive numerous solutions in special cases of three body problem. The Jacobi integral remains constant even though energy and momentum are not conserved separately (Haoze Tang, 2019). The motion of the test third body is restricted to a three-dimensional surface $H = -C/2 = const$, due to the existence of the Jacobi constant (Zotos, 2015, 2016).

The complete analytical solution of system (1) is unknown, the generation of trajectories in the scope of this problem requires the use of numerical integration. Upon linearization in the vicinity of the libration point, the solution of the equations of motion takes the form (Korneev, & Aksenov, 2020):

$$\begin{aligned} a_x - 2v_y - (1 + 2c_2)x = 0, \\ a_y + 2v_x - (1 - c_2)y = 0, \\ a_z + c_2 z = 0. \end{aligned} \tag{3}$$

Coefficient c_2 depends on the ratio of the masses of the Sun and the Earth and on the coordinates of the libration point used as the center of linearization. Solution of system (3) may be written as:

$$\begin{aligned} x(t) = A_1 k_2 e^{\lambda t} + A_2 k_2 e^{-\lambda t} + A_3 k_1 \cos(\omega t) + A_4 k_1 \cos(\omega t), \\ y(t) = -A_1 k_4 e^{\lambda t} + A_2 k_4 e^{-\lambda t} + A_3 k_3 \sin(\omega t) - A_4 k_3 \cos(\omega t), \\ z(t) = -A_5 k_5 \sin(\alpha t) - A_6 k_5 \cos(\alpha t). \end{aligned} \tag{4}$$

$A_1 - A_6$ continuously depend on the initial conditions, while $k_1 - k_5$, λ, ω, α depend only on the constant c_2. The solution (7) indicates the existence of center manifold ($A_1 = A_2 = 0$) containing periodical and quasi-periodical solutions as well as asymptotic stable ($A_1 = 0$, $A_2 \neq 0$) and unstable ($A_1 \neq 0$, $A_2 = 0$) manifolds. Nonlinear dynamics described by the equations (1) in the case of RTBP has a similar structure in the vicinity of libration point (Gomez, Masdemont & Mondelo 2003; Gomez et al., 2004).

The Circular Restricted Three-Body Problem is a Hamiltonian system. So, the canonical equations of the system in the CRTBP are (Sengupta & Singla, 2002; Vela, & Jerrold, 2004):

$$v_x = p_x + y; \tag{5}$$

$$v_y = p_y - x; \tag{6}$$

$$v_z = p_z; \tag{7}$$

$$\frac{dp_x}{dt} = +p_y - \frac{(1-\mu)(x+\mu)}{((x+\mu)^2+y^2+z^2)^{\frac{3}{2}}} - \frac{\mu(x+\mu-1)}{((x+\mu-1)^2+y^2+z^2)^{\frac{3}{2}}} \tag{8}$$

$$\frac{dp_y}{dt} = -p_x - \frac{(1-\mu)y}{((x+\mu)^2+y^2+z^2)^{\frac{3}{2}}} - \frac{\mu y}{((x+\mu-1)^2+y^2+z^2)^{\frac{3}{2}}} \tag{9}$$

$$\frac{dp_z}{dt} = -\frac{(1-\mu)z}{((x+\mu)^2+y^2+z^2)^{\frac{3}{2}}} - \frac{\mu z}{((x+\mu-1)^2+y^2+z^2)^{\frac{3}{2}}} \tag{10}$$

Most problems in several fields of sciences and other areas, have a nonlinear dynamic, and in the most cases these problems cannot be solved. The motion in the phase space is confined to a plane. Phase plane method is one of the most important analysis for study these phenomena, since there is usually no analytical solution for a nonlinear system. So, in this study, will also use this method.

3. Application of the Runge-Kutta-Fehlberg Method to the Three-Body Problem

The circular restricted three-body problem's set of three, second order equations of motion can be uncoupled into a set of six first-order nonlinear equations of motion that satisfy the equation (Langford, & Weiss, 2023):

$$\dot{x} = f(x), \tag{11}$$

where

$$x = (x_1, x_2, x_3, x_4, x_5, x_6), \tag{12}$$

and

$$f(x) = (f_1(x), f_2(x), f_3(x), f_4(x), f_5(x), f_6(x)). \tag{13}$$

Here x represents a point in the phase plane, and $\dot{x}$ is the velocity vector at that point (Destrez et al., 2019). By flowing along the vector field, a phase point traces out a solution $\boldsymbol{x}$(t), corresponding to a trajectory winding through the phase plane. Furthermore, the entire phase plane is filled with trajectories, since each point can play the role of an initial condition. For nonlinear systems, there's typically no hope of finding the trajectories analytically. Even when explicit formulas are available, they are often too complicated to provide much insight. Instead, will try to determine the qualitative behavior of the solutions. Our goal is to find the system's phase portrait directly from the properties of $f(x)$. Given a set of six initial conditions, $x(t_0)$, x may be evaluated at a given time t by numerically integrating the vector function $f(x)$ from t_0 to t (Langford, & Weiss, 2023; Destrez et al., 2019).

Numerical integrations of the three-body problem were first carried out near the begining of the twntieth century, and are now commonplace. For typical scattering events, or other short-lived solutions, there there is usually little need to go beyound common Runge-Kutta methods, provided that automatic step-size controlis adopted (Heggie, 2006). The basic generalization of the Runge-Kutta-Fehlberg (RKF) method is:

$$x_{n+1} = x_n \sum_{i=1}^{s} b_i k_i, \tag{14}$$

where

$$k_1 = hf(x_n, t_n) \tag{15}$$

$$k_2 = hf(t_n + c_2 h, x_n + a_{21} k_1) \tag{16}$$

...

$$k_s = hf\big(t_n + c_s h, x_n + a_{s1} k_1 + a_{s2} k_2 + \cdots + a_{s,s-1} k_{s-1}\big), \tag{17}$$

where x_n is a dependent variable, t_n is an independent variable, s is a number of stages, b_i, c_i and a_{ij} are coefficients that determined from Butcher tableau (Musielak, & Quarles, 2014).

The most common Runge-Kutta-Fehlberg implementation is Runge-Kutta-Fehlberg (RK F45). In this paper, the Runge-Kutta-Fehlberg (RKF 45) method was used to solve numerically the nonlinear system of differential equations of the three-body problem. This method is an algorithm in numerical analysis and the error in the solutions can be estimated and controlled by using a higher-order embedded method that allows for an adaptive step size to be determined automatically. The general form the Runge-Kutta-Fehlberg (RKF 45) is (Topputo, 2015, Banu, & Raju, 2021):

$$x_{n+1} = x_n + \frac{25}{216} k_1 + \frac{1408}{2565} k_3 + \frac{2197}{4104} k_4 - \frac{1}{5} k_5, \tag{18}$$

where n=1,2,3, …, and (Topputo, 2015, Banu, & Raju, 2021),

$$k_1 = hf(x_n, t_n), \tag{19}$$

$$k_2 = hf\left(x_n + \frac{1}{4} h, t_n + \frac{1}{4} k_1\right), \tag{20}$$

$$k_3 = hf\left(x_n + \frac{3}{8} h, t_n + \frac{3}{32} k_1 + \frac{9}{32} k_1\right), \tag{21}$$

$$k_4 = hf\left(x_n + \frac{12}{13} h, t_n + \frac{1932}{2197} k_1 - \frac{7200}{2197} k_2 + \frac{7296}{2197} k_3\right), \tag{22}$$

$$k_5 = hf\left(x_n + h, t_n + \frac{439}{216} k_1 - 8k_2 + \frac{3680}{513} k_3 - \frac{845}{4104} k_4\right), \tag{23}$$

$$k_6 = hf\left(x_n + \frac{1}{2} h, t_n - \frac{8}{27} k_1 + 2k_2 - \frac{3544}{2565} k_3 - \frac{1859}{4104} k_4 - \frac{11}{40} k_5\right). \tag{24}$$

The error in the solutions can be estimated and controlled by using a higher-order embedded method that allows for an adaptive step size to be determined automatically.

4. Results and Discussion

Equation (1) is used in the case when $m_3=0$ (RTBP), for lunar trajectories, to describe the path followed by a spacecraft or satellite in the Earth-Moon system. A spacecraft can follow various trajectories such as: Low Earth Orbit to Lunar Orbit (in this case a spacecraft can be launched from Earth and travel toward the Moon, adjusting its trajectory using gravitational assist or other maneuvers); Lagrange Points Orbits (in this case a spacecraft can also travel to one of the Lagrange points for observations or staging). Since the system of differential equations for many-body problems (as well as for the three-body problem, even in the limited case of $m_3=0$) is complex, exact solutions of CRTBP are generally not possible for arbitrary initial conditions. So instead of finding these solutions analytically, numerical integration method is used (Runge-Kutta-Fehlberg (45) method) to solve the equations of motion and simulate the trajectory of an object in the Earth-Moon system.

By choosing appropriate initial conditions, we can model the trajectory of a spacecraft traveling from Earth to the Moon, or any other lunar mission path. Initial Earth altitude is 200 km, initial angle between radial and earth-moon line is -90 degree. Initial flight path angle is 20 degrees. Final distance from the moon is 385157 km. Final relative speed (km/s) = 7.15542. Flight time is 6.165 days (round-trip) (Figure 1). Making a comparison, the trench trajectory of Apollo 11 of 1969, which normally differed from the one is presented, in many respects, required 3.04861 days to reach the point of insertion of the lunar orbit (Curtis, 2014). Figure 1a shows that the spacecraft returns near Earth to the position with coordinates (-6880.67, 14808.7) km. So, it is located approximately at an altitude of 14808.7 km above the Earth's surface. To get this result for the trajectory of a spacecraft in the Earth-Moon system is used the Runge-Kutta-Fehlberg (45) method to solve the earth-moon restricted three-body problem in the planar case ($z = 0$). Invariant manifolds play an important role in understanding the dynamics of the planetary systems, especially the behavior of trajectories near the Lagrange points. Figure 2 shows an unstable invariant manifold (trajectory in red) in the Earth-Moon system. Invariant manifolds are crucial for designing low-energy transfer orbits. For instance, spacecraft can use the stable manifolds near Lagrange points to reach distant regions in space, using minimal fuel by "slingshotting" off these manifolds. These manifolds help understand the long-term dynamics of the system, including the behavior of trajectories near equilibrium points, such as periodic orbits or quasi-periodic motion. The intersection of unstable and stable manifolds can lead to chaotic behavior in certain regions of phase space.

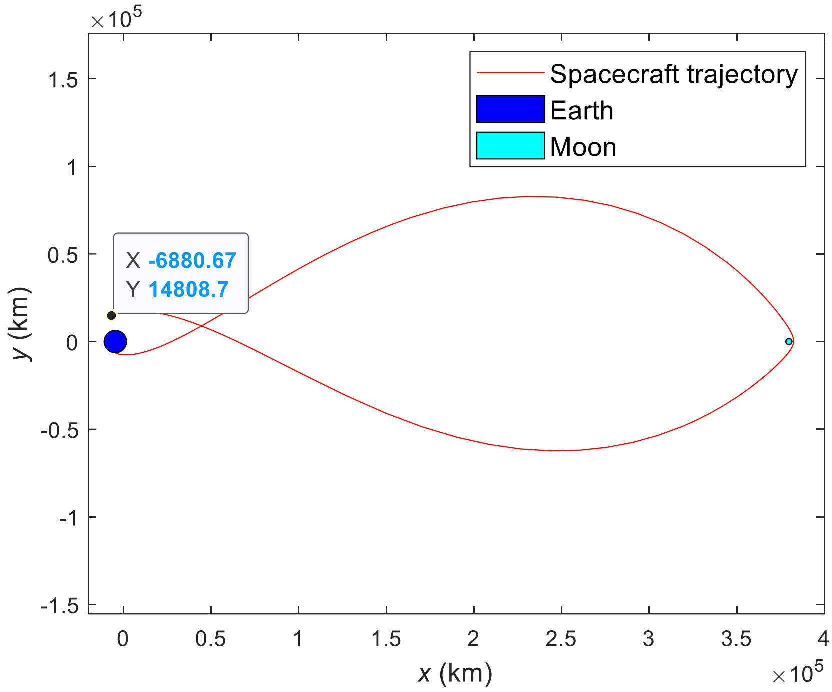

Figure 1. Translunar coast trajectory computed numerically from the restricted three-body differential equations using the RKF (45) method

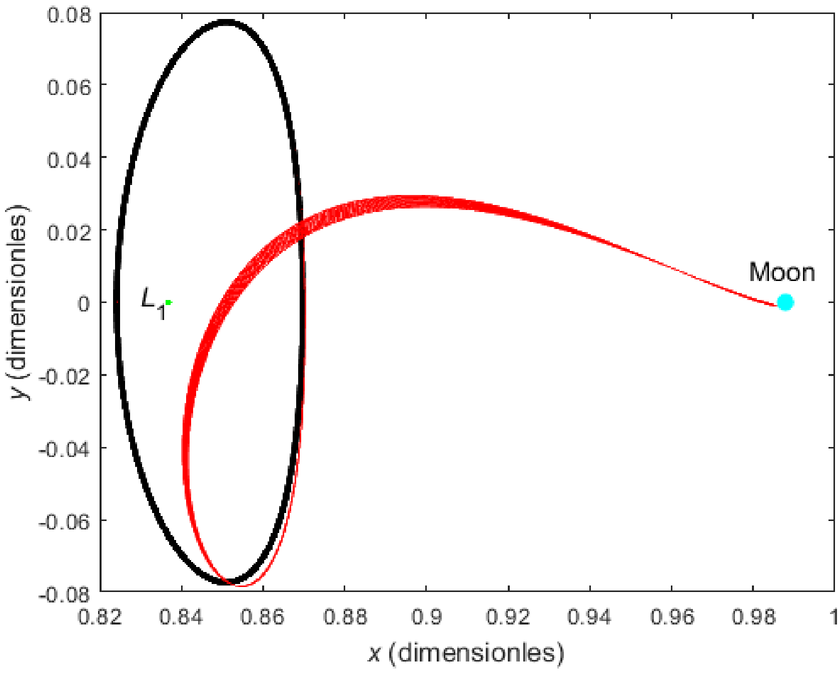

Figure 2. An unstable manifold in the Earth-Moon system

These intersections create complex dynamical structures, such as tangle patterns, which are important in understanding the global dynamics of the system. Tools like Poincaré sections and continuation methods are often used to visualize these manifolds and understand their global structure. To study complex chaotic systems, it is important to construct the Poincaré section.

The Poincaré section is used to analyze the dynamics of a system of complex differential equations by reducing it to a system of lower dimensional equations. To construct a Poincaré section, must graphically represent the dynamics of the test particle by fixing one of the coordinates in the rotating system, for example the x or y coordinate.

Let's focus on constructing a Poincaré section for the circular restricted three-body problem using MATLAB® 2024 b software.

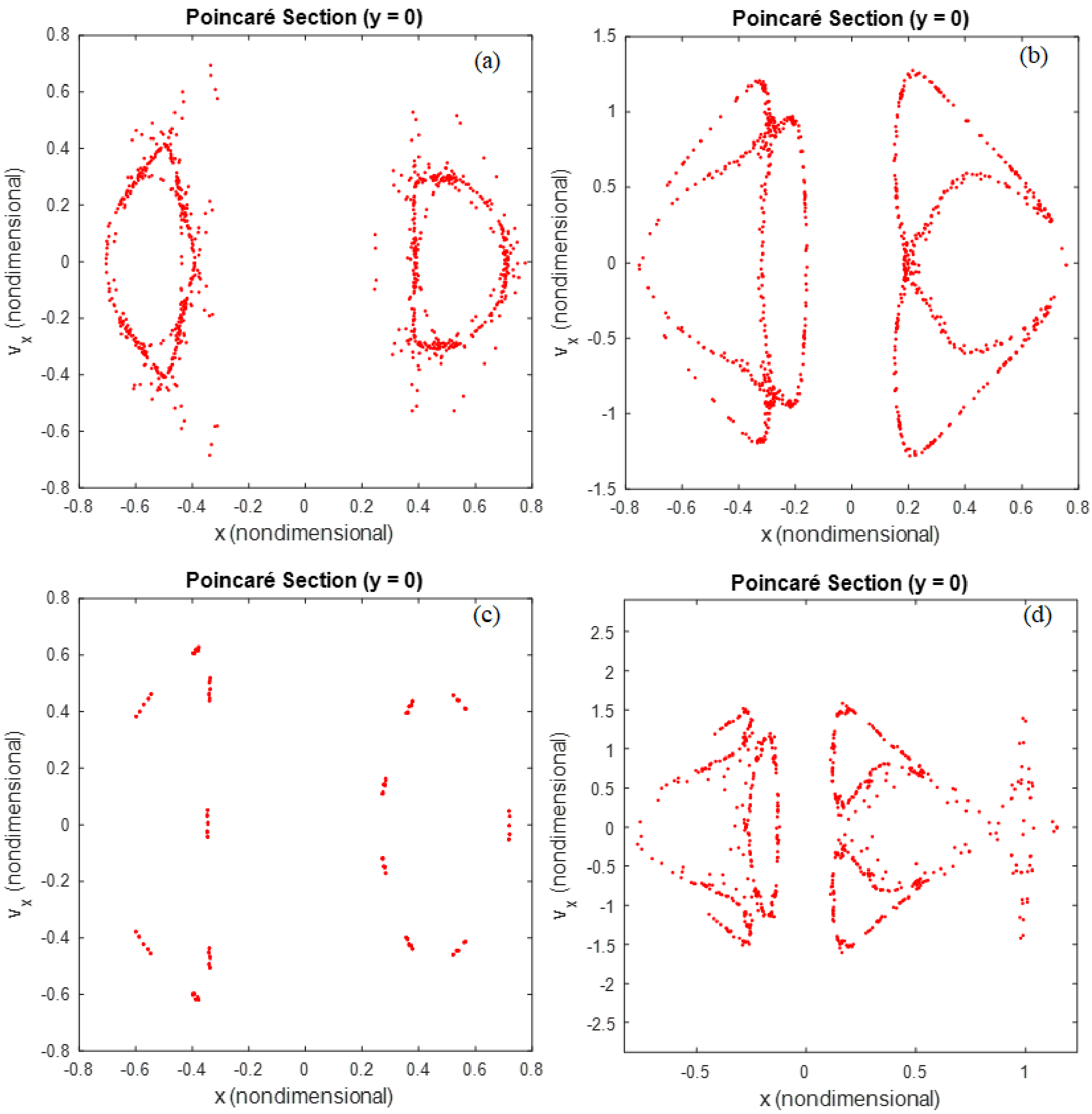

Figure 3. Poincaré section for μ=0.01215. (a) In this case the initial conditions are $x_0 = 0.75$, $y_0 = 0$, $v_{x0} = 0$, and $v_{y0} = 0.2$. The time of integration is 290 T. (b) Poincaré section for $x_0 = 0.75$, $y_0 = 0$, $v_{x0} = 0$, $v_{y0} = 0.1$ and the time of integration in this case is 200 T. (c) A Poincaré section for $x_0 = 0.72$, $y_0 = 0$, $v_{x0} = 0$, $v_{y0} = 0.17$ and t=70 T. (d) Poincaré section for $x_0 = 0.82$, $y_0 = 0$, $v_{x0} = 0$, $v_{y0} = 0.17$ and the time of integration 70T.

To create the Poincaré section the first need is to define the equations of motions for the three-body problem mentioned above in the section 2, to choose a coordinate to take the Poincaré section usually a plane (x, v_x) and simulate the system over time. Then record the intersections of the trajectory with the chosen plane or coordinate and finally plot the Poincaré section. Some results of the Poincaré section that calculated are shown in Figure 3. In this case, performed the calculations for the Earth-Moon system. Different initial conditions are used for the test particle of coordinates and velocities in the rotating frame. For the result in the Figure 3a chose the initial x-coordinate (in the rotating frame) is $x_0 = 0.75$, initial y-coordinate (in the rotating frame) is $y_0 = 0$, initial velocity in x-direction is $v_{x0} = 0$, initial velocity in y-direction is $v_{y0} = 0.2$. The time of integration is 290 T, where T is the orbital period (in arbitrary units). For the result in the Figure 3b chose the initial conditions: $x_0 = 0.75$, $y_0 = 0$, $v_{x0} = 0$, $v_{y0} = 0.1$. The time of integration is 200 T. In the Figure 3c use the initial conditions: $x_0 = 0.72$, $y_0 = 0$, $v_{x0} = 0$, $v_{y0} = 0.17$. The time of integration is 70 T. In the Figure 3d use the initial conditions: $x_0 = 0.82$, $y_0 = 0$, $v_{x0} = 0$, $v_{y0} = 0.17$. The time of integration is 70 T. Figure 4 shows the phase space in $\mathbb{R}^2$ for the Earth-Moon system. To reconstruct this phase space, wrote a code in MATLAB® 2024 b software, based on the algorithm of the Runge Kuta method, through which numerically integrated the system of differential equations (Hamilton's equations) (5-10).

Reconstructed the phase space for four cases. In the first case (Figure 4a) chose x_0=0; y_0=0.01; T=0.1; C=3.18. In Figure 4b used the values x_0=0; y_0=0.03; T=0.1; C=3.18. The third case is for x_0=1.2; y_0=0; T=20; C=3.1 (Figure 4c) and the fourth case is presented in Figure 4d for x_0=0.40455; y_0=0; T=30 and C=3.1731.

Scientific research in the field of exoplanets is very active and important. Humans have always been curious about the world beyond the solar system. Is there life out there on exoplanets? If so, how can we find this? Today, there are different methods and techniques for detecting exoplanets and searching for the possibility of life on them. In the present study, will apply the three-body problem in exoplanetary systems, as in the Solar system. A concrete case and a theoretical case are considered and analyzed.

Exoplanets have also been discovered in binary star systems. They can orbit around one of the stars or around two stars. Studies about this problem have increased a lot recently, especially in exoplanetary systems and nonlinear dynamics systems. For Kepler-35 system, the results showed that potentially habitable planets are formed in some simulations.

In new era technology of the computer, advanced numerical algorithm and numerical method, astronomical simulation and different methods, the field of study of exoplanet will be one of the most important targets, to study the enigmatic of extraterrestrial life.

In this study, found some different orbits in these systems. Some of these orbits are situated inside the habitable zone (HZ) and other outside. Also, found three types of hierarchical planet-binary configurations, S-type orbits (on orbits around the star), P-type orbits (orbits around binary stars) and T-type orbits (Trojan configurations). The basic configuration of the problem using in this research can have a real application in which the test particle may be considered as a "Trojan exoplanet", "Trojan exomoon" or "Trojan asteroid", moving in vicinity of two stars.

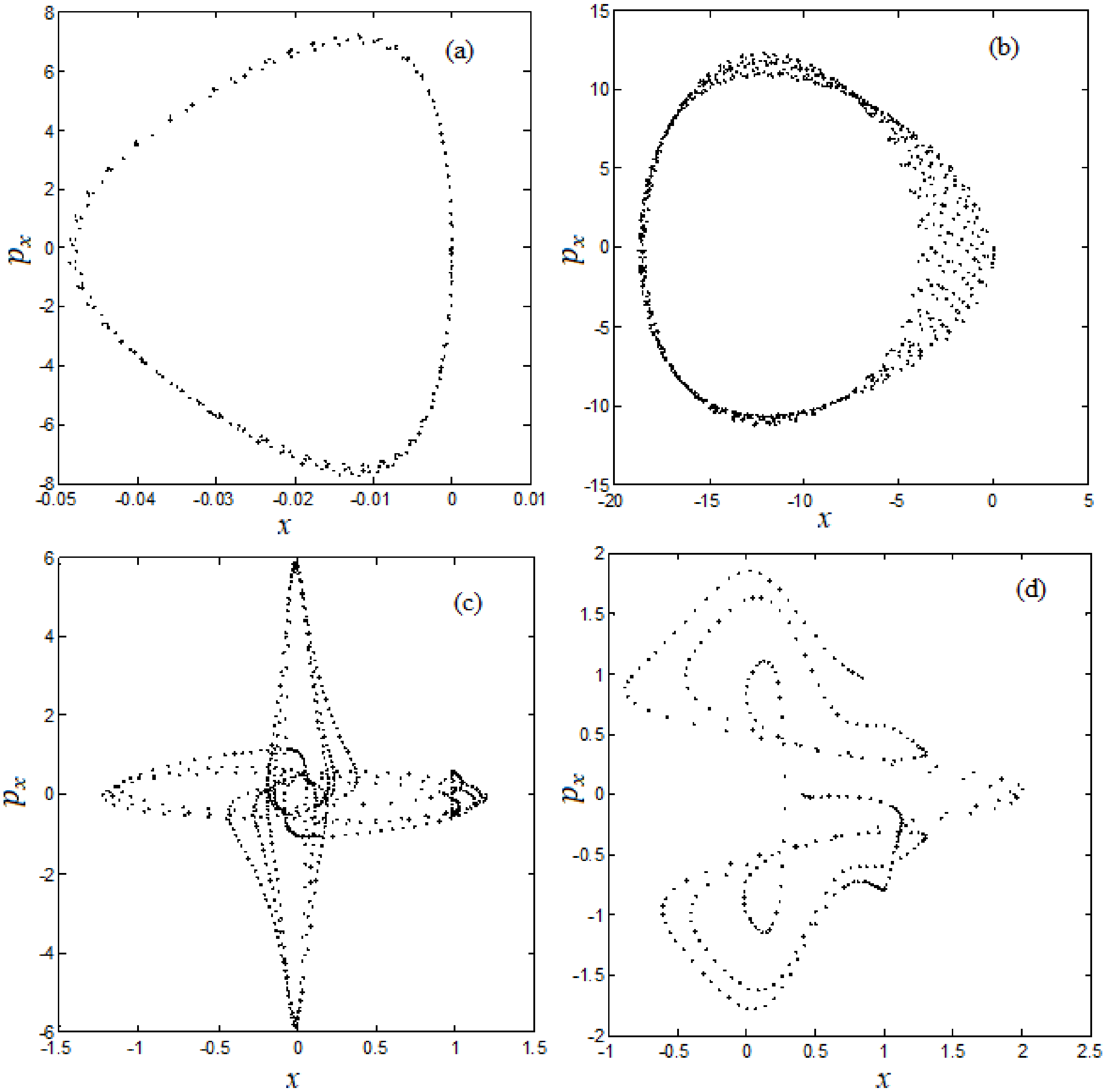

Figure 4. Phase space in $\mathbb{R}^2$ for the Earth-Moon system. (a) x_0=0; y_0=0.01; T=0.1; C=3.18; (b) x_0=0; y_0=0.03; T=0.1; C=3.18; (c) x_0=1.2; y_0=0; T=20; C=3.1; (d) x_0=0.40455; y_0=0; T=30; C=3.1731.

The graph of C (x, y) is shown in **Figure 5**. The energy C is plotted above each point (x, y) of the phase plane. The resulting surface is often called the energy surface for the system Kepler 35. For this system, the local minima of C project to centers in the phase plane. Contours of slightly higher energy correspond to the small orbits surrounding the stars. It is sometimes helpful to think of the flow as occurring on the energy surface itself, rather than in the phase plane. But notice-the trajectories must maintain a constant height C, so they would run around the surface, not down it (Strogatz, 1995). Also, **Figure 5** shows the position of Lagrange points for the system Kepler 35, the position of Kepler 35 A (the star in yellow) and the position of Kepler 35 B (the star in magenta).

Discoveries of exoplanets in binary star systems show that there are not only planets orbiting a single star. These discoveries lead to a great interest in better understanding the processes of planetary formation (Pilat-Lohinger, E., Sándorb, Zs., Gyergyovitsa M., and

Bazsó Á (2020)). Kepler-35 is a binary star system consisting of two stars, Kepler-35A and Kepler-35B and an exoplanet, Kepler-35b. These stars, have masses 0.9 M_S and 0.8 M_S respectively where M_S is the mass of the Sun, and, they are separated by 0.176 AU each other. Kepler-35b is a giant exoplanet (its mass is 0.127 M_J, where M_J is the mass of Jupiter) located at a distance 0.603 AU from the binary system and its period is 131.5 days in a P-type orbit. Numerical studies that have been done for the formation of this exoplanetary system show that the formation of rocky exoplanets in the habitable zone is high, and these planetary orbits are stable (Barbosa et al., 2020). The internal and external limits for the habitable zone (HZ) of the system Kepler 35 is 1.1 AU to 1.98 AU (Narrow HZ) and 0.89 AU to 2.09 AU (Wide HZ) (Barbosa et al., 2020). The habitable zone (CHZ) of this system is from 1.12 AU to 1.99 AU. The habitable zone EHZ is from 1.15 AU to 1.96 AU (Nikolaos G., Siegfried E., and Ian Dobbs-Dixon, 2021). In this paper, also considered the study of the dynamics of a test particle in a system with mass parameter 0.0147783251. In this system, will focus on findings S, P and T type trajectories. Also, chaotic trajectory. Figure 5b shows a P-type orbit (red orbit) around two stars. An astrophysical test object starts from the initial position with dimensionless coordinates x_0=2.81 and y=0. The integration time for this orbit is 120-time units and it is 0.4946 AU from the center of mass of the binary star system. The trajectory in black is chaotic. This trajectory shows how matter passes through the Lagrange point L_1 from the primary star A to the secondary star B. This point is important in the evolution of binary star systems because matter can flow from one Star (primary) to another (secondary) through the L_1 point. Type I supernova, for example, are caused by this flow of material through the L_1 point from a giant star to a compact white dwarf star, until so much material accumulates in the smaller star that a catastrophic explosion occurs.

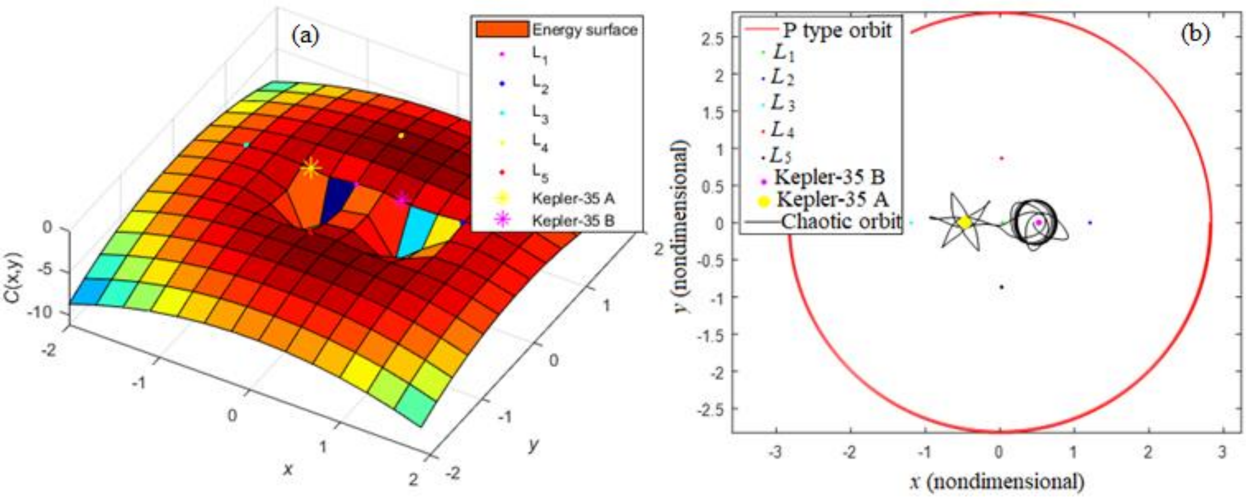

Figure 5. (a) Positions of Lagrange points, Kepler 35 A, Kepler 35 B and the graph of *C* (*x*, *y*). (b) Circular periodic orbit around binary (P-type orbit in red). Initial conditions for this orbit are x_0=2.81; y_0=0.00; time of integration is 120 unit of time; Jacobi constant is C=4.000000001452053. this orbit is approximately 0.4946 AU from the center of mass of the binary system.

Another important result in this aspect is presented in Figure 6a, a chaotic trajectory (the black trajectory) in a binary stellar system with mass parameter μ=0.0147783251. The blue orbit is a Zero-Velocity Curve (ZVC). The chaotic trajectory in black lies within the bounds defined by the ZVC.

Figure 6b shows several different orbits in this system. The orbit in black color is of type P. The orbits in pink color are two orbits of type T around the point L_4 and L_5 respectively. The yellow colored orbits are S-type orbits around the two stars A and B respectively.

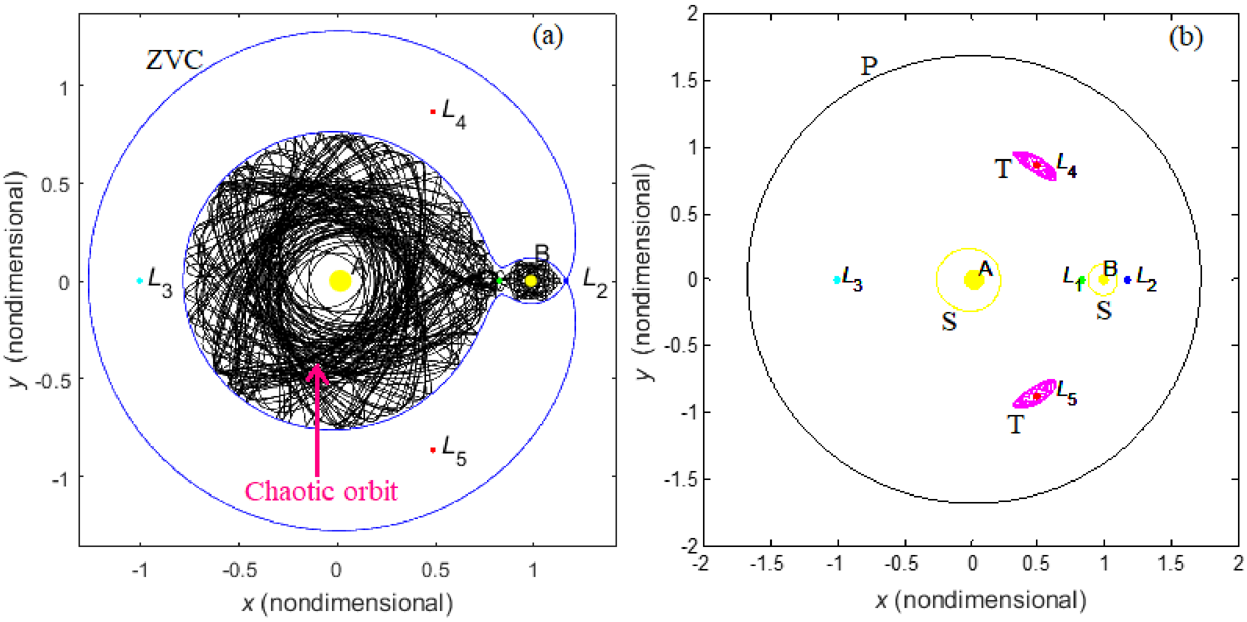

Figure 6. (a) Chaotic trajectory with μ=0.0147783251; x_0=0.835; y_0=0.00; T=500; and C=3.211482420202458. Trajectory in blue is a Zero-Velocity Curve (ZVC). (b) In this case chose x_0=1.72; y_0=0.00; T=11.55 and C=3.211482420202458for the P type orbit. For the orbit around the star A: x_0=0.225; y_0=0.00; T=0.6617; C=3.191812087771119. Around the star B: x_0=1.095; y_0=0.00; T=1.535; C=3.014773127695426. Around L_4 point: x_0=0.4878; y_0=0.86; T=230; C=3. Around L_5 point: x_0=0.4878; y_0=-0.86; T=230; C=3.

Conclusions

The "elements" of the orbit of the test particle in the three-body problem are not constants any more, but their variations are of order $\mathcal{O}(\mu)$. The system of differential equations of this problem (special case RTBP) provides an interesting and quite complex model for lunar trajectories, and spacecraft missions traveling to the Moon. If we know well the mathematics and physics of this problem, then we can correctly model the safe path that a spaceship or a space telescope should follow in space. This would help us plan accurately the lunar, interplanetary missions and maybe in the future also the interstellar missions. In most real applications, such as planning space missions to the Moon or other positions in space such as Lagrange points, numerical integration methods such as Runge-Kutta-Fehlberg (RKF 45), etc., are used to solve the system of differential equations of the problem that we have considered in this study. This way provides us with more accurate and practical solutions for the path that a test point (spaceship, space telescope or an astrophysical test object) will follow over time, especially in the presence of perturbations.

The above methods can also be applied to exoplanetary systems. From the other results of this study, conclude that there is a possibility that in the binary system (AB) with mass parameter μ=0.0147783251 there are astronomical objects performing P-type orbits around two stars, S-type orbits around star A and B, respectively, and T-type orbits around the Lagrange points L_4 and L_5.

References

Barbosa et al. (2020). Earth-size planet formation in the habitable zone of circumbinary stars. *MNRAS 494*, 1045–1057. https://doi.org/10.1093/mnras/staa757

Bertachini et al. (2013). Mathematical Methods Applied to the Celestial Mechanics of Artificial Satellites 2013. *Mathematical Problems in Engineering, 2013,* Article ID 854317. Hindawi Publishing Corporation. http://dx.doi.org/10.1155/2013/854317

Borcherds P. H. (1996). The restricted gravitational three-body problem trajectories associated with Lagrange fixed points. *Eur. J. Phys. 17*, 63–70.

Celleti, A. (2006). Stability Problems in Celestial Mechanics. *Encyclopedia of Mathematical Physics*. Elsevier Ltd.

Chenciner A., Montgomery R. (2000). A remarkable periodic solution of the three-body problem in the case of equal masses. *Annals of Mathematics. Second Series. 152*(3), 881–902. arXiv:math/0011268. doi:10.2307/2661357. JSTOR 2661357. S2CID 10024592.

Curtis H. D. (2014). *Orbital Mechanics for Engineering Students* (3rd ed.). Elsevier Ltd. ISBN–13: 978-0-08-097747-8.

Destrez et al. (2019). Rendezvous Strategies in the Vicinity of Earth-Moon Lagrangian Points. *Frontiers in Astronomy and Space Sciences, 5,* Article 45. https://doi.org/10.3389/fspas.2018.00045.

Gomez et al. (2004). Connecting orbits and invariant manifolds in the spatial restricted three-body problem. *Institute of Physics Publishing, Nonlinearity 17*, 1571–1606, PII: S0951-7715(04)67794-2.

Gomez G, Masdemont J and Mondelo J. (2003). Libration point orbits: a survey from the dynamical point of view (pp 311–372).

Govind S. K. and Himalaya S. (2019). An introduction to the classical three-body problem from periodic solutions to instabilities and chaos. *Resonance 24*(1), 87-114.

Heggie D. C. (2006). Gravitational N-Body Problem (Classical). *Encyclopedia Mathematical* (pp. 575-582). https://doi.org/10.1016/B0-12-512666-2/00003-1

Hristov et al., (2023). Three-body periodic collisionless equal-mass free-fall orbits revisited. arXiv:2308.16159v1 [physics.class-ph]. https://doi.org/10.1007/s10569-023-10177-w.

Hudomal A. (2015). New periodic solutions to the three-body problem and gravitational waves (PDF). Master of Science Thesis at the Faculty of Physics, Belgrade University. https://www.scl.rs/theses/msc_ahudomal.pdf.

Hysa, A. (2024). A study of the nonlinear dynamics inside the exoplanetary system Kepler-22 using MATLAB® software. *EUREKA: Physics and Engineering, 2,* 3–12. https://doi.org/10.21303/2461-4262.2024.003257

Hysa, A. (2024). Non-linear dynamics of a test particle near the Lagrange points L4 and L5 (Earth-Moon and Sun-Earth case). *EUREKA: Physics and Engineering, 1,* 3–10. https://doi.org/10.21303/2461-4262.2024.002949

Hysa, A. (2024). Study of the resonant motion of a test particle inside Kepler 69 using circular restricted three body problem. *Technology Transfer: Fundamental Principles and Innovative Technical Solutions*, 34-37. https://doi.org/10.21303/2585-6847.2024.003563.

Hysa, A., Peqini, K., Hafizi, M. (2024). A Study of the linear and non-linear dynamics of a Trojan Astrophysical object within Exoplanetary system HD 126053. *Journal of Natural Science, 36*. https://jns.edu.al/a-study-of-the-linear-and-nonlinear-dynamics-of-a-trojan-astrophysical-object-within-exoplanetary-system-hd-126053/

Jacobi, Carl G. J. (1836). Sur le movement d'un point et sur un cas particulier du problème des trois corps. *Comptes Rendus de l'Académie des Sciences de Paris*, ***3,*** 59–61.

Korneev, A and Aksenov, S., (2020), Calculation of libration point orbits in the circular restricted three-body problem. *Journal of Physics: Conference Series*, *1740*(2021), 012019. IOP Publishing. doi:10.1088/1742-6596/1740/1/012019.

Krishnaswami G. S., and Senapat, H. (2019). An Introduction to the Classical Three-Body Problem. From Periodic Solutions to Instabilities and Chaos. *RESONANCE*, January 2019. https://doi.org/10.1007/s12045-019-0760-1 .

Lagrange J. L. (1772). Essai sur le Problème des Trois Corps. *Oeuvres de Lagrange, 6*, 229-292. Paris: Gauthier-Villars, 1873.

Langford, A., Weiss, L. M. (2023). A Dynamical Systems Approach to the Theory of Circumbinary Orbits in the Circular Restricted Problem. arXiv:2302.00580v1 [astro-ph.EP] 1 Feb 2023. https://doi.org/10.3847/1538-3881/acb7df

Lee, J., & Ahn, J. (2021). Successive optimization framework for weak stability boundary trajectory design. In *Ascend 2021* (p. 4152).

Lee, J., & Ahn, J. (2022). Poincaré filter for trajectory design in multi-body regime. In *Aiaa scitech 2022 forum* (p. 1129).

Lee, J., & Ahn, J. (2024). Low-thrust resonance gravity-assist trajectory design for lunar missions. *Journal of Spacecraft and Rockets*, 1–10.

Lei and Xu (2013). High-order analytical solutions around triangular libration points in the circular restricted three-body problem. *MNRAS 434,* 1376–1386. doi:10.1093/mnras/stt1099.

Lizy-Destrez et al. (2019). Rendezvous Strategies in the Vicinity of Earth-Moon Lagrangian Points. *Front. Astron. Space Sci. 5,* 45. doi: 10.3389/fspas.2018.00045.

Lorenz E. (1963). Deterministic non-periodic flow. *Journal of the Atmospheric Sciences 20*(2), 130–141.

More C. (1993). Braids in classical dynamics. *Physical Review Letters, 70*(24), 3675–3679. doi:10.1103/PhysRevLett.70.3675, PMID 10053934.

Murray D., Dermott, S. F (1999). *Solar System Dynamics* (1st ed.). Cambridge University Press. https://assets.cambridge.org/97805215/72958/sample/9780521572958wsn01.pdf.

Musielak, Z.E., Quarles, B. (2014). The Three-Body Problem. *Reports on Progress in Physics, 77,* Article ID: 065901. https://iopscience.iop.org/article/10.1088/0034-4885/77/6/065901.

Newton I. (1687). *Philosophiæ naturalis principia mathematica (Mathematical Principles of Natural Philosophy).* London: Royal Society Press.

Nikolaos G., Siegfried E., and Ian Dobbs-Dixon (2021). Circumbinary Habitable Zones in the Presence of Giant planet. https://doi.org/10.3389/fspas.2021.640830

Pilat-Lohinger, E., Sándorb, Zs., Gyergyovitsa M., and Bazsó Á (2020). Planets in Binary Stars. Published on: February 14, 2020. http://dx.doi.org/10.22323/1.342.0010

Poincaré, J. H. (1890). Sur le probleme des trois corps et les equations de la dynamique. Divergence des series de m. Lindstedt. *Acta Math. 13,* 1–270.

Rebeca S. Ribeiro, R.S., de Melo, C.F., Prado, A.F.B.A. (2022). Trajectories Derived from Periodic Orbits around the Lagrangian Point L1 and Lunar Swing-Bys: Application in Transfers to Near-Earth Asteroids. *Symmetry, 14,* 1132. https://doi.org/ 10.3390/sym14061132

Roman, R., Szücs, C. I. (2011). Regularization of the Three-Body Problem Using” Similar” Coordinate Systems. *Rom. Astron. J., 21*(2).

Roman, R., Szücs, C. I. (2012). New regularization of the restricted three-body problem. *Romanian Astron. J., 22*(2), 135–144.

Roman, R., Szücs, C. I. (2014). A family of zero-velocity curves in the restricted three-body problem. *Astrophys Space Sci 352*, 481–49. https://doi.org/10.1007/s10509-014-1988-6

Sengupta P., Singla P. (2002). *An analysis of stability in the restricted three-body problem*. MEEN 689 PROJECT, Graduate Students, Department of Aerospace Engineering Texas A&M University.

Stone N. C., Leigh N. W. (2019). A statistical solution to the chaotic, non-hierarchical three-body problem. *Nature 576*(7787), 406–410.

Szebehely, V. (1967). *Theory of Orbits*. Academic Press, New York.

Szücs, C. I. (2023). Overview–regularization and numerical methods in Celestial Mechanics and Dynamical Astronomy. *Romanian Astron. J., 33*(1–2), 37–56. DOI 10.59277/RoAJ.2023.1-2.03.

Tang, H.Z. (2019). Koopman Reduced Order Control for Three Body Problem. *Modern Mechanical Engineering, 9*, 20-29. https://doi.org/10.4236/mme.2019.91003

Vela A. L. V., Jerrold E. M. (2004). Time-frequency analysis of the restricted three body problem: Transport and resonance transitions. https://www.cds.caltech.edu/~marsden/bib/2004/01-VeMa2004/VeMa2004.pdf.

Xiaoming L., Yipeng J., Shijun L. (2017). The 1223 new periodic orbits of planar three-body problem with unequal mass and zero angular momentum. arXiv:1709.04775v1 [nlin.CD] 13 Sep 2017.

Zotos, E. E. (2016). Investigating the planar circular restricted three-body problem with strong gravitational field. arXiv:1708.05300v2 [nlin.CD] 17 Sep 2017. https://arxiv.org/abs/1708.05300

Zotos, E. E. Classifying orbits in the restricted three-body problem. arXiv:1511.04881v1 [physics.space-ph] 16 Nov 2015.